Injection Modulation in Coupled Laser Oscillators

VALERIO ANNOVAZZI LODI AND SILVANO DONATI, MEMBER, IEEE

Abstract—**Injection modulation is the effect observed when laser oscillation is perturbed by an injected signal below the threshold of locking. In this regime the oscillation becomes a wave modulated in frequency as well as in amplitude. The modulation envelope has a characteristic waveform which depends on the amplitude and phase of the injected signal.**

Starting from the Lamb's equations for a dual-mode oscillator, we develop a theory of the injection modulation and calculate the waveforms in amplitude and frequency. The treatment applies both to the external injection into a laser and to the case of mutual coupling between two modes.

Experimental results for a dual mode He-Ne laser are found to be in good agreement with the theory. It is pointed out how the injection modulation effects are appreciable even at very weak levels of injected amplitudes, e.g., down to 10^{-5} with respect to the oscillation field amplitude.

I. Introduction and Analysis of the Frequency Beating

LASER injection locking is a well-known phenomenon [1]-[3] which is encountered in several applications either as an active or undesired mechanism of interaction between two oscillators. Generally, injection locking can also be regarded as a special case of a coupled regime of oscillation for two sources.

Manuscript received January 12, 1980. This work was supported by the CNR.

The authors are with the Istituto di Elettronica, Università di Pavia, Pavia, Italy.

Coupling levels below the threshold of frequency locking do not amount to negligible effects, but on the contrary give rise to a conspicuous modulation of the laser oscillation, both in frequency and in amplitude. This modulation, when detected as a beating of the two coupled oscillations, is transferred from optical frequencies down to electrical frequencies where it exhibits a highly characteristic waveform containing information on amplitude and phase of the complex coupling coefficient (properly defined) between the two oscillators.

The analysis we present in this paper is suitable as a description of the weak coupling phenomena, i.e., both for external injection into the laser and for mutual coupling between two modes oscillating in the same source. The main results also apply to other types of Van der Pol oscillators [4], and indeed the same modulation waveforms have been observed in microwave oscillators [5]. Lastly, we show how to perform, through the injection modulation, an indirect measurement of the coupling coefficient down to levels of 10^{-5}.

Injection modulation is an effect contained in the Lamb equations description of two laser oscillations E_1 and E_2 in the presence of mutual coupling. Letting $\Gamma = \gamma \exp ie$ for the coupling rate, i.e., the rate of change of one field due to the other field, Lamb's equations are written as

$$\dot{E}_1 = \left(- \frac{\nu_1}{2Q} + \alpha_1 - \beta_1 E_1^2 - \vartheta_1 E_2^2 \right) E_1 - \gamma_2 E_2 \cos (\psi_2 - \psi_1 + e_2) \quad (1)$$

0018-9197/80/0800-0859$00.75

$$\dot{\psi}_1 = \nu_1 + \dot{\varphi}_1$$

$$= \Omega_1 + \frac{\nu_0 - \nu_1}{\Delta\nu}(\alpha_1 - \beta_1 E_1^2 - \vartheta_1 E_2^2)$$

$$- \gamma_2 \frac{E_2}{E_1} \sin(\psi_2 - \psi_1 + \epsilon_2) \tag{2}$$

$$\dot{E}_2 = \left(-\frac{\nu_2}{2Q} + \alpha_2 - \beta_2 E_2^2 - \vartheta_2 E_1^2\right) E_2$$

$$- \gamma_1 E_1 \cos(\psi_1 - \psi_2 + \epsilon_1) \tag{3}$$

$$\dot{\psi}_2 = \nu_2 + \dot{\varphi}_2$$

$$= \Omega_2 + \frac{\nu_0 - \nu_2}{\Delta\nu}(\alpha_2 - \beta_2 E_2^2 - \vartheta_2 E_1^2)$$

$$- \gamma_1 \frac{E_1}{E_2} \sin(\psi_1 - \psi_2 + \epsilon_1) \tag{4}$$

where, in addition to the usual terms [2], [6], [7] for uncoupled oscillations, the last terms in the amplitude and phase equations describe the interchange of a fraction $\gamma \exp i\epsilon$ of the fields, from one oscillator to the other. This set applies to a dual mode Zeeman laser and to a ring laser [2], [3], in which the internal coupling is usually mutual and symmetrical; on the opposite end, it also describes the external injection into a laser, as in a master-slave two-laser system.

We start with the symmetrical coupling assumption, i.e., $\gamma_1 = \gamma_2 = \gamma$ and $\epsilon_1 = \epsilon_2 = \epsilon$, and will treat the external injection case later on.

As suggested by experimental evidence and confirmed below, we now take the amplitudes E_1 and E_2 of the oscillating fields as constant. This amounts to neglect, as a first approximation, the effects of amplitude modulation with respect to those of frequency modulation, and to ignore possible hysteresis effects. Then, letting $\dot{E}_1 = \dot{E}_2 = 0$, we can solve the set (1)–(4) for $\dot{\psi} = \dot{\psi}_1 - \dot{\psi}_2$, i.e., the beating frequency of the two oscillations, as

$$\dot{\psi} = A + B \sin(\psi + \psi_A). \tag{5}$$

Equation (5) is a standard form of the locking equation [2], [3], [6], in which A is the frequency difference of the oscillations in unperturbed conditions, and B is the locking frequency. The expressions of frequency and phase terms are found under the condition of moderate detuning $(\nu_0 - \nu)/\Delta\nu \ll 1$ (which helps to simplify and is usually satisfied), to be

$$A = \Omega_1 - \Omega_2 - \frac{\nu_1 - \nu_0}{2Q}\frac{\nu_1}{2Q} + \frac{\nu_2 - \nu_0}{2Q}\frac{\nu_2}{2Q} \tag{6}$$

$$B = \gamma\left[\left(\frac{E_2}{E_1}\right)^4 + \left(\frac{E_1}{E_2}\right)^4 + 2\cos 2\epsilon\right]^{1/2} \tag{7}$$

$$\psi_A = \operatorname{atan}\left[\frac{(E_2/E_1)^2 - 1}{(E_2/E_1)^2 + 1}\tan\epsilon\right]. \tag{8}$$

As it is well known [1], [3], the frequency locking of the two oscillations is obtained by letting $\dot{\psi} = 0$ in (5). This gives the locking condition $B \geq A$ and a phase difference locked at $\psi = -\psi_A - \arcsin(A/B)$.

The region of weak coupling or injection is that below threshold, i.e., for $B < A$, for which we can get a solution of (5) in the form

$$\psi(t) = \arcsin\frac{\sin\phi(t) - K}{1 - K\sin\phi(t)} - \psi_A \tag{9}$$

where

$$K = B/A$$

is a coupling ratio, and

$$\phi(t) = A(1 - K)^{1/2}\, t + \arcsin K \tag{10}$$

is the phase associated with the mean frequency difference.

From (9) one finds that the beating frequency oscillates between $\omega_{max} = A + B$ and $\omega_{min} = A - B$, with a mean value $\omega_M = A(1 - K^2)^{1/2}$. As the locking threshold is approached from the weak coupling side, the mean frequency ω_M progressively decreases, though the frequency excursion $\omega_{max} - \omega_{min}$ is constant.

The beating waveform obtained at a photodetector, i.e., $\cos\psi(t)$, is correspondingly modified from a pure sinusoid to a strongly distorted double-pulse waveform.

From a numerical evaluation of (9), we find the diagrams of Figs. 1 and 2; the trend with respect to K, from very weak coupling ($K \to 0$) to locking threshold ($K \to 1$) is clearly pictured. The dependence from the phase factor ψ_A is displayed in Fig. 2 for the range 0–90°, and it can be seen that the main

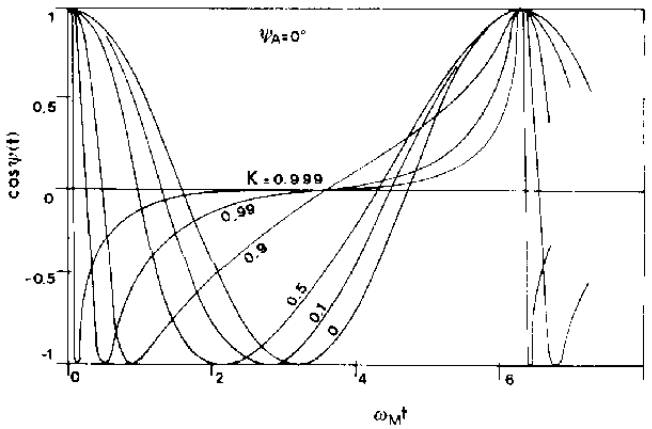

Fig. 1. Beating waveforms of the injection modulation below the threshold of locking, for some values of the coupling ratio K and for $\psi_A = 0$.

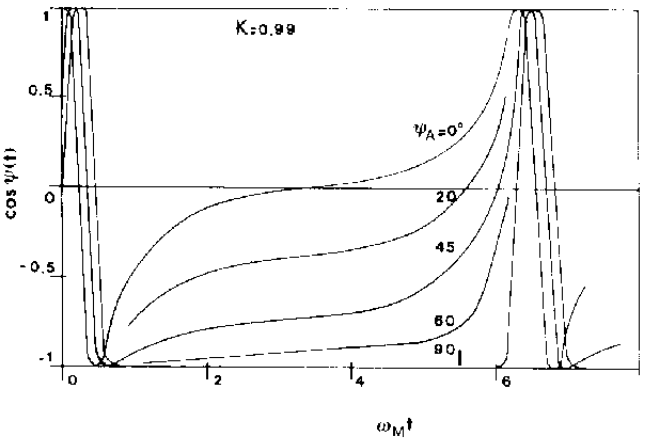

Fig. 2. The same as in Fig. 1, with ψ_A as a parameter and $K = 0.99$.

feature involved is the half period ordinate (plateau) of the waveform. For ψ_A in the range of 90-360°, curves similar to those of Fig. 2 are found, simply by a congruent transformation—a rotation of 180° of the diagrams for the fourth quadrant (so that the plateau is at positive ordinates), and a time inversion for the second and third quadrants of the diagrams corresponding to the first and fourth ones.

II. Amplitude Modulation Waveforms

Going back to the field amplitude equations (1) and (3), we can use the time dependence found above for the phase difference $\psi_1 - \psi_2$ to obtain a first-order evaluation of the amplitude modulation.

In the symmetrical coupling assumption, by expanding $E_1(t)$ and $E_2(t)$ around the constant stationary values E_{10} and E_{20} (which satisfy the equations for $\gamma = 0$), we get at first order for $e_1(t) = E_1(t) - E_{10}$ and $e_2(t) = E_2(t) - E_{20}$

$$\dot{e}_1 = -2\beta_1 E_{10}^2 e_1 + 2\vartheta_1 E_{10} E_{20} e_2 - \gamma E_{20} \cos(\psi - \epsilon) \quad (11)$$

$$\dot{e}_2 = -2\beta_2 E_{20}^2 e_2 + 2\vartheta_2 E_{10} E_{20} e_1 - \gamma E_{10} \cos(\psi + \epsilon). \quad (12)$$

This set can be reduced to a single second-order differential equation

$$\ddot{e}_1 + \dot{e}_1 (\beta_1 E_{10}^2 + \beta_2 E_{20}^2) + 4 e_1 (\beta_1 \beta_2 - \vartheta_1 \vartheta_2) E_{10}^2 E_{20}^2 = F(t) \quad (13)$$

where the forcing term is

$$F(t) = -2\gamma\beta_2 E_{20}^3 \cos(\psi + \epsilon) - 2\gamma\vartheta_1 E_{10}^3 \cos(\psi - \epsilon) + \gamma E_{20} \dot{\psi}(t) \sin(\psi + \epsilon). \quad (14)$$

Since the poles of the left-hand side of (13) are found to be located at frequencies larger than those contained in the spectrum of the term $F(t)$ (for the usual values of its parameters), the solution is written by inspection in the form

$$e_1(t) = [4(\beta_1\beta_2 - \vartheta_1\vartheta_2) E_{10}^2 E_{20}^2]^{-1} F(t)$$

where the term in square brackets is the product of the two poles of (13). Substituting for $F(t)$ from (14), we get

$$e_1(t) = e_{10} \cos[\psi(t) + \psi_B] \quad (15)$$

where

$$e_{10} \simeq \gamma/2\beta_1 E_{10} \approx \gamma E_{10}/2\alpha \quad (16)$$

and

$$\psi_B = \operatorname{atan}\left(\frac{E_{20}}{E_{10}} \tan\epsilon\right) - \frac{\pi}{2} \quad (17)$$

and similarly for e_2 (with the sign of phase ϵ changed).

Note how e_1 and e_2 have a form similar to that of the frequency beating $\cos\psi(t)$. Therefore, they belong to the same family of curves as in Figs. 1 and 2, and a simple change of parameters is required to describe the amplitude modulation waveforms, by means of the plots of Figs. 1 and 2, by letting ψ_A be replaced by $\psi_A + \psi_B$ [see (15)]. The modulation depth is small for $\gamma \ll 2\alpha$, a condition of low-level coupling which justifies the above assumptions.

An interesting representation of the amplitude transient is supplied by the state diagram of Fig. 3, which is obtained by writting the expressions of field intensities $I_1 = E_1^2$ and $I_2 = E_2^2$

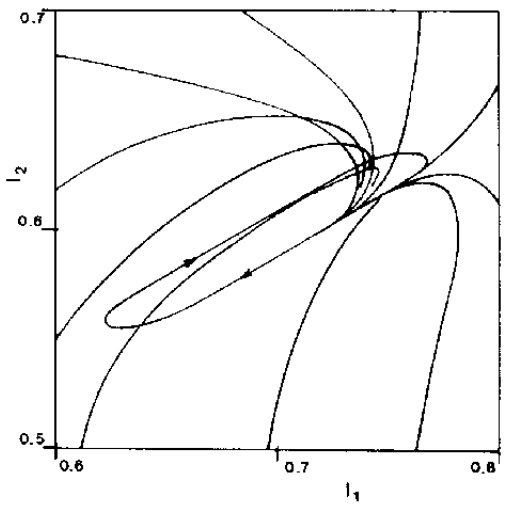

Fig. 3. State diagram of mode intensities. All paths, starting from different points, enter the limit cycle nearly in the same region determined by the initial phase difference ψ_0. Normalized parameter values: $K = 0.5$; $A = 1$; $\gamma = 0.25$; $\alpha_1 = (\nu_1/2Q) = \beta_1 = 2$; $\alpha_2 = (\nu_2/2Q) = 3$; $\beta_2 = 4$; $\vartheta_2 = \vartheta_1 = 1$; $\epsilon = \psi_0 = 0$.

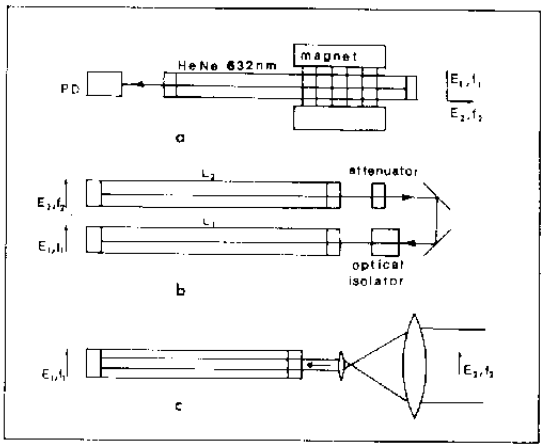

Fig. 4. (a) Schematic of a dual-mode laser for mutal coupling analysis and (b) of two-lasers systems with external injection of L_2 and L_1, and (c) of a laser receiving a remote signal.

with the aid of (1) and (3), and plotting the solution in parametric form for the time variable. The limit cycle corresponding to the oscillating fields intensities (see Fig. 3) is reached in about one period of $\psi(t)$ from the points external to the cycle. The diagram is illustrative of a typical He-Ne two-mode laser, with moderate coupling of the modes.

III. External Injection

So far, we have considered a two-way symmetrical coupling, i.e., that was found in a two-mode laser [see Fig. 4(a)]. To treat the case of external injection into a laser system, such as in Fig. 4(b) or (c) we let $\gamma_1 = 0$ and $\vartheta_1 = \vartheta_2 = 0$ in (1)-(4), so that

$$\dot{E}_2 = 0 \qquad \dot{\psi}_2 = \text{constant}.$$

Again assuming $\dot{E}_1 = 0$, we find the beating frequency $\dot{\psi} = \dot{\psi}_1 - \dot{\psi}_2$ expressed in the same form as (5), where the param-

eters are now modified as follows:

$$A = \Omega_1 - \dot{\psi}_2 - \frac{\nu_1 - \nu_0}{2Q} \frac{\nu_1}{2Q} \tag{18}$$

$$B = \gamma_2 E_2/E_1 \tag{19}$$

$$\psi_A = -\epsilon. \tag{20}$$

Similar to the discussion of the symmetrical case, as K ranges from 0 to 1, the oscillation will increasingly exhibit frequency and amplitude modulation until the synchronization regime is reached because of the injected signal. The beating waveform $\cos \psi(t)$ is still given by the same expression as (9) and it belongs to the family depicted in Figs. 1 and 2, and the amplitude modulation is similarly given to first order by (15)-(17).

It is interesting to note how, because of the frequency modulation produced in E_1 by the injected signal E_2, the frequency difference $\dot{\psi} = \dot{\psi}_1 - \dot{\psi}_2$ has a larger deviation than that eventually contained in E_2 under the form of a slowly varying frequency signal $\dot{\psi}_2$. Thus, from the expression of ω_M, the gain is found to be

$$d\dot{\psi}/d\dot{\psi}_2 = (1 - K^2)^{-1/2}$$

and is always greater than unity. Moreover, since the ratio $d\dot{\psi}_1/d\dot{\psi}_2$ of the frequency deviations of the perturbed mode with respect to the injected signal is $\approx K^2/2$, after a heterodyne detection and a frequency-to-amplitude conversion, the obtained signals dS_1 and dS_2 associated with $d\dot{\psi}_1$ and $d\dot{\psi}_2$ are in the ratio

$$dS_1/dS_2 = \frac{K^2}{2} \frac{E_1}{E_2}$$

which can be greater than unity. This amounts to an extrinsic amplification supplied by the injection modulation process.

IV. Beating Modulation Measurements

Experiments have been performed with a commercial He-Ne laser, an internal mirror, and a 0.5 mW unit modified to operate in a single-mode stabilized frequency [8]. A splitting of the atomic line was obtained by applying a transverse magnetic field (200 gauss) on a short section of the plasma tube. Thus, the oscillation is split into two orthogonally polarized modes [6], [8], whose frequency difference due to pulling effects is in the range of 10-100 kHz. This dual-mode laser corresponds to the setup of Fig. 4(a), and allows one to evaluate the symmetrical mode-coupling modulations. The beating signal was detected by a photodiode analyzing the modes through a polarizer, oriented at 45° in respect to mode polarizations.

The experimental waveforms obtained at the photodiode output are compared in Fig. 5 with theoretical curves calculated from (9).

Note how the agreement is good over a full family of curves for the obtained values $\gamma = 0.12$ MHz and $\epsilon = 74°$. The various waveforms were obtained at decreasing levels of detuning of the stabilized laser, what amounts to a decrease in the factor A from the top to the bottom in Fig. 5. The factor B was not a constant because of the dependence of E_2/E_1 on the detuning; however, its variation is quite consistent with a constant value of γ as calculated according to the procedure outlined in the next section. A similar remark applies to ψ_A, whose values are consistent with a constant ϵ. The jitter in the last waveform of Fig. 5 is due to small perturbations of the setup.

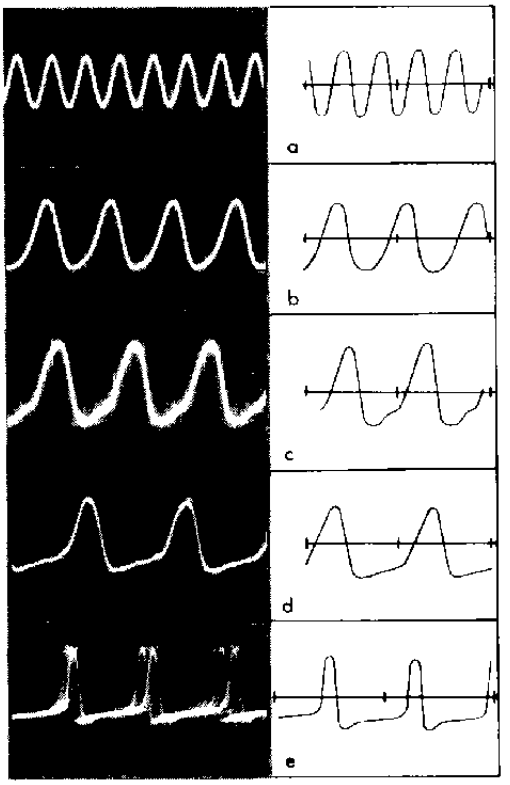

Fig. 5. Experimental beating waveforms of frequency modulation due to a symmetrical coupling in a dual-mode He-Ne laser. In the right side, the calculated waveforms are plotted for comparison. Detuning decreases from top to bottom traces, and correspondingly the frequency difference ω_M ranges from 47 to 7.5 kHz (time scale: 100 μs/div). The coupling ratio $K = B/A$ for curves a-e is: 0.33, 0.78, 0.85, 0.90, and 0.97. For $K < 0.33$ and $50 < \omega_M < 100$ kHz, the waveform is nearly a sinusoid. The parameter ψ_A is evaluated from curves b-e as 49°, while B ranges from 100 to $200 \cdot 10^3$ rad/s.

Amplitude modulation waveforms were detected by orienting the polarizer in front of the photodiode parallel to one mode, and the measurement supplied a small value of the modulation index (0.01), as expected, since $\gamma \ll 2\alpha$ (for $\alpha \simeq 5$ MHz and $\gamma = 0.12$ MHz); also, the amplitude modulation waveforms were consistent with those predicted by (16)-(18). The external injection was also investigated experimentally with the configuration of Fig. 4(b), in which an optical isolator allows injection of L_1 into L_2 and not vice versa.

The isolator is also required to avoid the retroreflection, at the front mirror of L_1, of the beam of L_2 back into its cavity. This would give rise to a three-mirror laser cavity which is governed by the so-called induced-modulation regime [8]. Indeed, the difference in (3) and (4) would be that in the last term E_1 should be replaced with E_2 and ψ_1 with $2Ks$, the optical path-length of the external mirror. As a consequence, the cavity field E_2 would carry amplitude and frequency modulations terms of the form $\cos 2Ks$ and $\sin 2Ks$. It has been shown [8] that these terms allow an interferometric measurement of the distance s. Later, the induced modulation effect has been found to be responsible for the amplitude fluc-

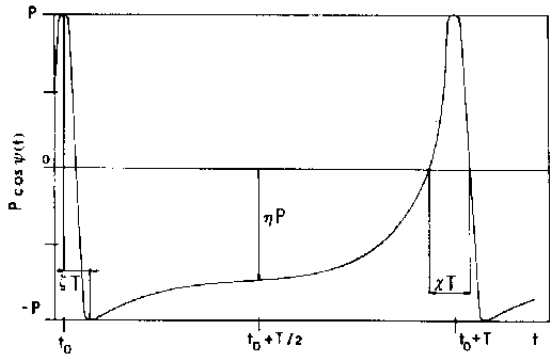

Fig. 6. Typical beating waveform and definition of parameters η, ζ, and χ.

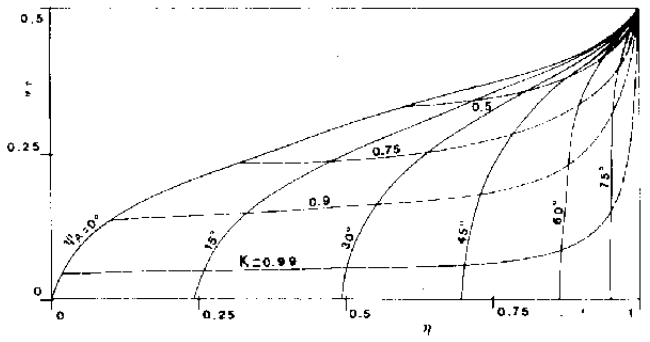

Fig. 7. (a) The transformation from shape parameters η and ζ to coupling ratio K and phase rt term A. (b) Changing ψ_A into $90^\circ - \psi_A$, the plot also describes ψ_A and K with χ (instead of ζ) as a parameter.

tuations due to backscattering and remote reflections from a fiber into a single-mode semiconductor laser [9].

The extinction of our isolator (a few percent) was insufficient to render induced-modulation effects negligible: however, the beating of the two stabilized lasers, forcing one frequency to scan around the other, was observed to display the family of waveforms of Figs. 1 and 2 with ψ_A drifting rapidly over the range of 0-360° due to setup vibrations.

V. Method of the Coupling Coefficient Measurement

From the waveforms of Fig. 5, the coupling ratio K and the phase term ψ_A can be inferred by an indirect *a-posteriori* method, i.e., by comparing a family of curves as was done in the previous section. Alternatively, we can measure, from the experimental waveform, two shape parameters like the half-period amplitude η and the duty cycle ζ (or χ) as defined in Fig. 6; their dependence from K and ψ_A is easily determined as follows:

$$\eta = -\cos\left[\arcsin\frac{f(\psi_A + K)}{1 + Kf(\psi_A)} - \psi_A\right] \tag{21}$$

$$\zeta = \frac{1}{2} - \frac{1}{2\pi}\left(\arcsin f(\psi_A) + \arcsin f - \psi_A\right) \tag{22}$$

$$\chi = \frac{1}{2} - \frac{1}{2\pi}\left[\arcsin\frac{\cos\psi_A + K}{f(\psi_A + \pi/2)} + \arcsin\frac{-\cos\psi_A + K}{f(\psi_A - \pi/2)}\right] \tag{23}$$

with

$$f(\psi_A) = \frac{\sin\psi_A + K}{1 + K\sin\psi_A}$$

and from the plots of Fig. 7 one can directly determine the coupling ratio K and phase factor ψ_A associated with a measured waveform. For the best accuracy, the duty factor to be used is ζ in the range of $0 < \psi_A < 60^\circ$ and χ in the range of $60^\circ < \psi_A < 90^\circ$.

A further step is provided by the diagrams of Fig. 8 which allows one to compute modulus and phase of the coupling rate $\Gamma = \gamma \exp i\epsilon$ once ψ_A and $K = B/A$ have been determined, and one knows the frequency difference A and amplitude ratio E_1/E_2 in unperturbed conditions. The use of the diagram is as follows: from ψ_A and E_1/E_2 we find ϵ as the top-left corner

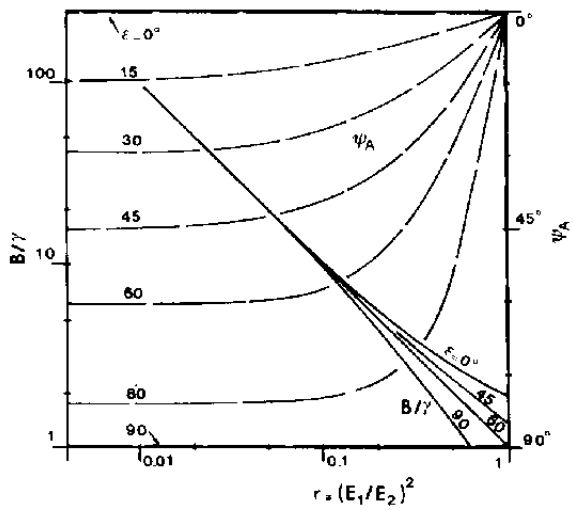

Fig. 8. Transformations of the coupling rate $\Gamma = \gamma \exp i\epsilon$ to B and ψ_A, as a function of the intensity ratio $r = (E_1/E_2)^2$.

parameter, and then B/γ can be found by reentering the diagram with r and ϵ (bottom right corner); finally, γ is given by $AK/(B/\gamma)$.

In Fig. 7, ψ_A is limited to the range of 0-90°, for which $\eta < 0$; for $\eta > 0$, ψ_A should be changed to $-\psi_A$; in the case of the time inversion of the beating curves of Figs. 1 and 2, ψ_A should be changed in $180^\circ - \psi_A$ ($\eta < 0$) or into $\psi_A + 180^\circ$ ($\eta > 0$). In Fig. 8, the diagram is periodic over 90° for both ψ_A and ϵ, which always lie in the same quadrant, while in the B/γ diagram, ϵ or $-\epsilon$ are periodic with period 180°. For $r > 1$, the entry $1/r$ gives B/γ and $-\psi_A$, respectively.

We are now in a position to evaluate the coupling coefficient which governs the injection modulation. Since $\Gamma = \gamma \exp i\epsilon$ is a rate of change, it is suitable to consider the coupling coefficient $\Gamma' = (2L/c)\Gamma$ which is adimensional and represents the coupling per pass. In the experimental setup of Fig. 4(a), Γ' is a measure of the coupling effects such as internal scattering, depolarization at the mirrors, and magnetic field misalignment all resulting in a mixing of the modes.

In the above experiment, we have adjusted the magnet axis so as to compensate, as far as possible, the other coupling effects. In these conditions, the measurement of coupling coefficient $\Gamma' = \gamma' \exp i\epsilon$ yields $\gamma' = 2.2 \times 10^{-4}$ and $\epsilon = 74^\circ$. By an estimate of instrumental accuracy, it appears that the

sensitivity limit is around $\gamma' = 10^{-5}$ in our experimental arrangement. Obviously, relatively large coupling deliberately introduced into the laser, for example, by a separate off-axis magnet or an external quater-wave plate and mirror, were easily measurable up to a factor of the order of $\gamma' = 10^{-2}$ as a limit of incipient nonlinear effects.

References

[1] C. J. Buzek, R. J. Freiberg, and M. L. Skolnick, "Laser injection locking," *Proc. IEEE*, vol. 61, pp. 1411–1431, Oct. 1973.

[2] F. Aronowitz and J. Collins, "Lock-in and intensity phase interactions in the ring laser," *J. Appl. Phys.*, vol. 41, pp. 130–141, 1970.

[3] W. J. Tomlison and R. L. Fork, "Properties of gaseous optical masers in weak axial magnetic fields," *Phys. Rev.*, vol. 164, pp. 466–483, 1967.

[4] W. C. Lindsey, *Synchronization Systems in Communication and Control*. Englewood Cliffs, NJ: Prentice-Hall, 1972, p. 240.

[5] P. Arcioni and G. Conciauro, "Automodulation in mutually coupled microwave oscillators," *Alta Frequenza*, vol. 46, pp. 400–421, 1977.

[6] M. Sargent III, W. E. Lamb, Jr., and R. L. Fork, "Theory of a Zeeman laser," *Phys. Rev.*, vol. 164, pp. 450–465, 1967.

[7] W. E. Lamb, Jr., "Theory of an optical maser," *Phys. Rev.*, vol. 134, pp. 1429–1450, 1964.

[8] S. Donati," Laser interferometry by induced modulation of cavity field," *J. Appl. Phys.*, vol. 49, pp. 495–498, 1978.

[9] O. Hirota and Y. Suematsu, "Noise properties of injection lasers due to reflected waves," *IEEE J. Quantum Electron.*, vol. QE-15, pp. 142–149, Mar. 1979.

Valerio Annovazzi Lodi was born in Novara, Italy, on November 7, 1955. He received the degree in Electronic Engineering from the University of Pavia, Pavia, Italy in 1979.

He is the recipient of a Selenia Fellowship awarded to University of Pavia for a research program on electrooptic instrumentation. His main research interests involve laser interferometry and solid state devices.

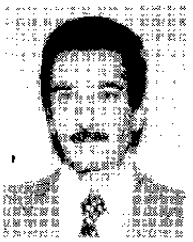

Silvano Donati (M'75) was born in Milano, Italy, on August 19, 1942. He received a degree in physics from Università di Milano in 1966.

From 1966 to 1975 he worked at CISE, Milano, first on nuclear electronics and photodetector noise, and later on electrooptic instrumentation, active L^3TV, and fiberoptics. In 1971 he was appointed a Lecturer of Electronic Engineering at Università di Pavia, Pavia, Italy, and in 1975 he became a Professor of Electro-Optics Systems. His main research interests include laser interferometry, noise in detectors and in detection processes, induced modulation in oscillators, and electrooptic measurements. He is the author of over 35 papers.

Prof. Donati is a member of the American Physical Society, the Optical Society of America, and the Association of Electrical and Electronic Engineers of Italy (AEI).